Materials and Design 88 (2015) 58–68

Contents lists available at ScienceDirect

Materials and Design

journal homepage: www.elsevier.com/locate/jmad

Friction welding of mild steel and titanium: Optimization of process parameters and evolution of interface microstructure

T.N. Prasanthi [a,1], C. Sudha [a], Ravikirana [b], S. Saroja [a,*,2], N. Naveen Kumar [c], G.D. JanakiRam [c]

[a] Microscopy and Thermo-Physical Property Division, Physical Metallurgy Group, Metallurgy and Materials Group, Indira Gandhi Centre for Atomic Research, Kalpakkam, 603102, India
[b] Homi Bhabha National Institute — IGCAR, India
[c] Department of Metallurgical and Materials Engineering, Indian Institute of Technology-Madras, Chennai-600 036

ARTICLE INFO

Article history:
Received 9 May 2015
Received in revised form 25 August 2015
Accepted 27 August 2015
Available online 1 September 2015

Keywords:
Mild steel
Titanium
Friction welding
Heat treatment
Intermetallic phases
JMatPro

ABSTRACT

The present investigation deals with the efforts to form a defect free bonded interface between mild steel (MS) and titanium (Ti) using the rotation friction welding process. The conditions were optimized based on several trials by varying friction welding parameters like frictional force, upset force, burn-off length and rotational speed. It has been established that only fine FeTi particles formed in isolated regions at the interface of 'as welded' MS/Ti joints. The evolution of interface microstructure has been studied by diffusion annealing heat treatments in the temperature range of 500–800 °C for a duration of 100 h. Plastic deformation during friction welding reduced the recrystallisation temperature of MS. The variation in microchemistry was measured across the weld interface, which was used as input to predict the formation of various phases and the consequent change in the mechanical properties using the JMatPro® software. Intermetallics were present only as fine isolated particles in bcc-Fe matrix at the interface even after heat treatment at 800 °C for 100 h. The growth kinetics was found to be much slower in friction welded joints as compared to diffusion bonded and explosive clad joints.

1. Introduction

Evaluation of the weldability and microstructural stability of iron (Fe) and titanium (Ti) based dissimilar joint is important due to its application in the spent fuel reprocessing plant of fast breeder reactors [1,2]. Earlier investigations on 304L SS/Ti–5Ta–2Nb dissimilar joint fabricated using a solid state welding process (explosive cladding) revealed the formation of undesirable reaction zones at the interface during post-clad heat treatments [3]. Growth kinetics of these zones was observed to be high in explosive clads as compared to diffusion bonded joints [4]. This was attributed to the severe deformation of the two materials during explosive cladding, resulting in the formation of high number density of defects that acted as short circuit diffusion paths for the alloying elements. In order to obtain a fundamental understanding on the role of defects and alloying elements in accelerating/retarding the kinetics of formation of diffusion zones, a binary Fe–Ti system has been taken up for study. The joint has been fabricated employing both equilibrium and non-equilibrium (explosive cladding) processes and compared. Due to limitations in obtaining plates of pure iron with minimum dimensions of 500 × 500 mm required for explosive cladding, the joints have been fabricated with commercially available mild steel (MS) (Fe–0.14C) and grade-2 Ti.

Fabrication of MS–Ti diffusion couple is a challenge due to the (1) limited mutual solubility of Fe and Ti [5], (2) tendency for the formation of brittle intermetallic phases at the interface (diffusivity of Fe (in hcp Ti): 5×10^{-15} m^2/s and Ti (in bcc Fe): 5.5×10^{-14} m^2/s at 900 °C) [6], (3) large difference in their thermal expansion coefficients (Fe: 12 μm/m/K and Ti: 8.6 μm/m/K) [7], and (4) formation of thick oxide scales. The approach adopted in literature has been to initially form a bonded interface between Fe and Ti through the application of both high temperature (800–950 °C) and pressure (3 MPa for 0.5 to 1.5 h) in diffusion bonding set up followed by diffusion annealing heat treatments [8]. Diffusion bonding technique is effective to obtain Fe–Ti joints with adequate bond strength. However, formation of a continuous layer of intermetallic phases parallel to the joint interface could not be avoided even under optimized experimental conditions [9,10]. This poses problems when the main objective of the investigation is to study the diffusivities of elements in solid solutions rather than in ordered intermetallic phases. Friction welding is a promising solid state welding technique where by appropriate selection of process parameters it is possible to obtain joints with adequate bond strength and control the formation of secondary phases [11,12].

The aim of the present investigation was to optimize the process parameters for rotation friction welding of MS and Ti and characterize the microstructure and properties of the weld. Further, the evolution of interface microstructure and its effect on the properties due to

* Corresponding author.
E-mail address: saroja@igcar.gov.in (S. Saroja).
[1] Ph.D. Scholar, Homi Bhabha National Institute (HBNI), Department of Atomic Energy (DAE).
[2] Head, Microscopy & Thermo-Physical Property Division and Professor, HBNI, DAE

http://dx.doi.org/10.1016/j.matdes.2015.08.141
0264-1275/

diffusion annealing in the temperature range of 500–800 °C for duration of 100 h has been studied. The variation in microchemistry across the interface has been evaluated using Electron Probe Micro Analysis (EPMA) which forms the input for predicting the various phases that can form at the interface and consequent change in the mechanical properties using JMatPro, a materials modeling software [13]. This investigation forms part of a study on interface and diffusion behavior for a comparison of these under equilibrium and non-equilibrium conditions, provided by the explosively clad MS/Ti joints.

2. Materials and methods

Chemical compositions of the plates used in the present study are given in Table 1. From MS and grade-2 Ti plates of dimension 1000 × 500 × 20 mm and 1000 × 500 × 12 mm respectively, rods of 10 mm diameter and 100 mm length were fabricated for friction welding. The contact surfaces were well polished up to a mirror finish to eliminate any surface roughness. During friction welding, the MS rod was kept in the static mode and the Ti rod was rotated and moved towards MS to avoid the higher extent of flash due to high deformation of Ti. Through a combination of compressive force and high temperature (~1425 °C generated during the process — for 304SS/MS) [14] the materials were joined together by plastic deformation. Several trial runs were carried out by varying the process parameters such as frictional force (FF), upset force (UF), burn off length (BOL) and the rotational speed (R). The selection of parameters for friction welding is based on literature available for Fe–Ti alloy systems [12,15]. It is understood that BOL and R are important parameters which dictate the interface microstructure. The selection of BOL of 2 and 3 mm in the present study is supported by Meshram et al. [12] and Dey et al. [15] and who have reported good bonding at 2 and 3 mm respectively when BOL was varied in the range of 2–5 mm. In the present study the rotational speed was varied in the range of 750–1500 rpm and found that 1000 rpm is optimum based on interface microstructure. This is also supported by studies in similar systems namely Ti-304 SS and Fe–Ti where R was maintained as 1500 and 1000 rpm respectively. The selection of frictional force and upset force is based on literature in similar systems [12,16].

After friction welding, the flash (materials that were expelled out at the interface) was removed by subsequent machining. Cross section of the bonded specimens having a dimension of 10 × 10 mm was extracted for further analysis. After grinding and polishing of the specimens by standard metallographic procedures, final polishing was carried out using smooth alumina suspension. To reveal the microstructure, MS side of the joints was etched with nital (5 ml HNO_3 in 95 ml Methanol) and Ti side with Kroll's reagent (4.5 ml conc. HNO_3 + 0.5 ml HF in 45 ml of distilled water). Based on the metallurgical analysis of all specimen fabricated during the trial runs, optimum friction welding parameters were identified.

The specimen fabricated under optimized condition was then sealed under vacuum in quartz tubes and subjected to diffusion annealing heat treatments in the temperature range of 500–800 °C for duration of 100 h. After heat treatment, the specimens were air cooled and prepared using the same procedure as detailed above for microstructural characterization.

Microstructural characterization was carried out using Leica MeF4A optical microscope and scanning electron microscope (XL 30 ESEM of M/s FEI) at an operating voltage of 30 kV. Leitz microhardness tester

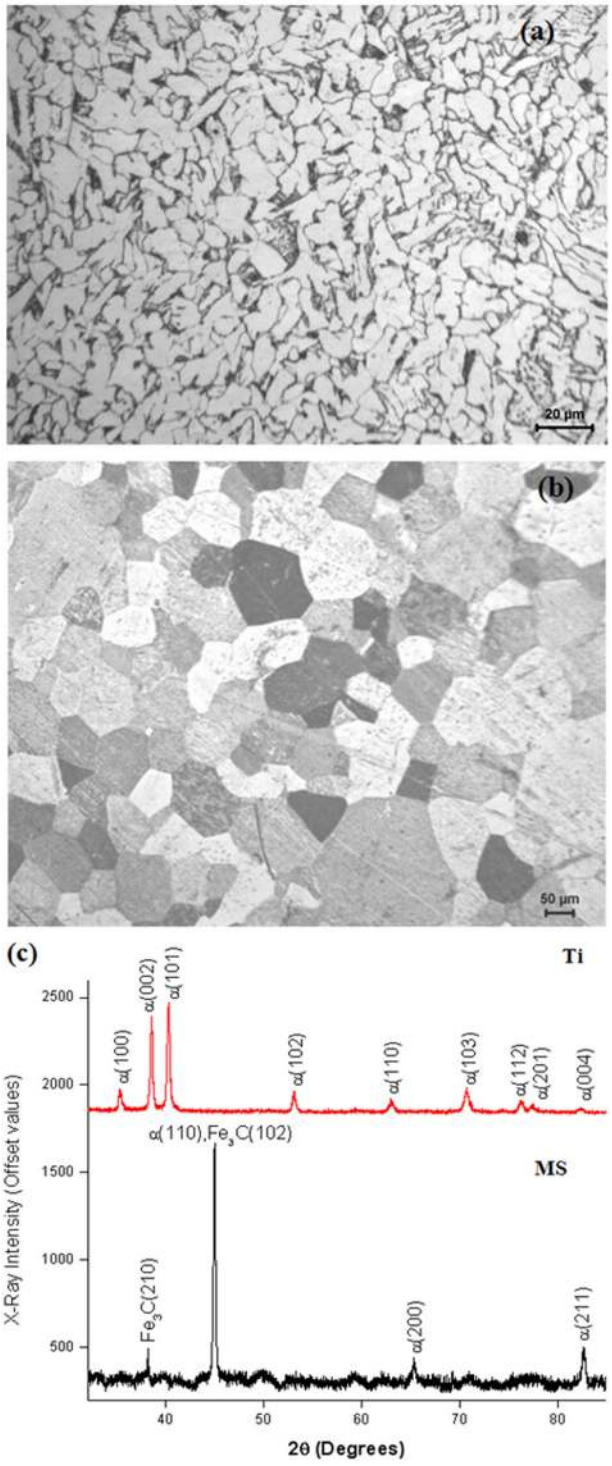

Fig. 1. Optical micrograph of a. mild steel showing ferrite + pearlite structure b. grade-2 Ti showing equiaxed α grains and c. XRD pattern obtained from MS and Ti before friction welding.

Table 1
Chemical composition (in wt%) of the materials used in the present study.

Material	C	S	P	Mn	Si	Al	Fe	N	H	O	Ti
Mild steel	0.141	0.032	0.03	0.786	0.138	0.028	Bal.	–	–	–	–
Grade-2 Ti	0.023	0.03	–	–	–	0.1	0.02	0.012	0.001	0.06	Bal.

Table 2
List of process parameters varied for friction welding.

Trail run no.	Frictional force (FF) tonnes	Upset force (UF) tonnes	Burn off length (BOL) mm	Rotational speed (R) rpm
1	0.8	1.6	3	750
2	0.8	1.6	3	1000
3	0.8	1.6	3	1500
4	0.8	1.6	2	1000
5	1	2	3	750
6	1	2	3	1000
7	1	2	3	1500
8	1	2	2	1000

with an applied load of 100 g was used for microhardness measurements. Each hardness value is an average of five readings obtained from regions with similar microstructure. Crystallographic changes at the weld interface were studied using INEL XRG-3000 X-ray diffractometer with Cu K_α radiation at a glancing incidence angle of 5°. The detector used for the XRD analysis is a curved sensitive position detector with an angular range (2θ) and step size of 10–100° and 0.012° respectively.

Microchemical characterization of the joints was carried out using Cameca SX-Five electron probe micro analyzer (EPMA). Concentration profiles were obtained across the MS/Ti weld joints both in the 'as welded' condition and after thermal exposure. An accelerating voltage of 20 kV and beam current of 20 nA was used for the analysis. Diffracting crystals used for the analysis were LLiF for Fe Kα, LPET for Ti Kα and PC2 for C Kα. Quantitative analysis was performed by comparing the intensities of Kα radiation of the elements obtained from the sample with that of the metallic pure elemental standards. The measured X-ray intensities were corrected for atomic number, absorption and fluorescence effects to obtain accurate chemical composition for the elements of interest. The composition obtained across the weld interface was used as the input to predict the probable phases that would form at the interface using JMatPro® (version 6.2). A CALPHAD based approach is adopted in predicting the mole fraction of the various phases. Consequent change in the mechanical properties of the weld joints due to presence of these secondary phases was also evaluated using this software [13]. To validate the simulation conditions, initially the room temperature tensile properties of MS and Ti plates were estimated and compared with experimental data. Grain size, estimated volume fraction of phases was used to fix the simulation conditions. Further, the approach was extended to the estimation of mechanical properties of the weld joints.

For transmission electron microscopy (TEM) investigations, electron transparent 3 mm diameter thin foils were specifically extracted from the bonded interface. The thin foils were then mechanically polished followed by jet thinning. For jet thinning, a solution of 10% $HClO_4$ and 90% CH_3OH was used as the electrolyte at an operating voltage of 15 V, current of 40–60 mA at a temperature of −30 °C. Electron microscopy studies were carried out using PHILIPS CM200 TEM fitted with a SDD energy dispersive spectrometer (EDS) at an operating voltage of 200 kV. Selected Area Diffraction (SAD) patterns were analyzed using ImageJ software and compared with standard ICDD data for confirmation of various phases.

3. Results

3.1 Optimization of friction welding parameters:

Fig. 1a–c show the optical microstructure and consolidated XRD pattern of the MS and Grade-2 Ti used in the fabrication of the friction welds. As expected, MS had both ferrite and pearlite ($\alpha + Fe_3C$) phases with an average hardness of 154 ± 5 VHN. Pearlite appeared as a dark etched region in the optical micrograph (Fig. 1a), while Grade-2 Ti exhibited equiaxed grains (Fig. 1b) with an average hardness of 210 ± 7 VHN corresponding to well annealed Ti. Analysis of the XRD pattern (Fig. 1c) confirmed the presence of only α-ferrite and hcp (α) phase in 'as received' plates of MS and Ti respectively.

Eight trial welds were fabricated by changing the process parameters as listed in Table 2. Back scattered electron images (BSE) obtained from the cross section of these are shown in Fig. 2a to h with the microhardness profiles superimposed on the micrographs. Optimization of the friction welding parameters has been made by monitoring the change in microstructure and average hardness of base materials with reference to the 'as received' values and the interface microstructure with respect to irregularities and pores. The variation in hardness was observed to be higher for MS than Ti in all cases. Signatures of deformation up to a distance of ~50 μm was generally observed on the Ti side due to its low yield and ultimate tensile strength (260 and 325 MPa respectively) as compared to mild steel (MS) (285 and 445 MPa respectively). Porosities were predominant when the rotational speeds were increased beyond 1000 rpm (Fig. 2c and g) due to insufficient diffusion of the elements across the interface. The average hardness at the interface was maximum (~352 VHN) for the weld fabricated using the highest FF, UF and BOL = 2 mm (Fig. 2h). The microstructure in Fig. 2b shows absence of porosities, no deformation on Ti side and relatively low increase in hardness (~309 VHN) at the interface, which is considered as a favorable structure. This weld joint corresponds to parameters of FF = 0.8 tonnes, UF = 1.6 tonnes, BOL = 3 mm and R = 1000 rpm. Hence, these parameters are considered as optimum

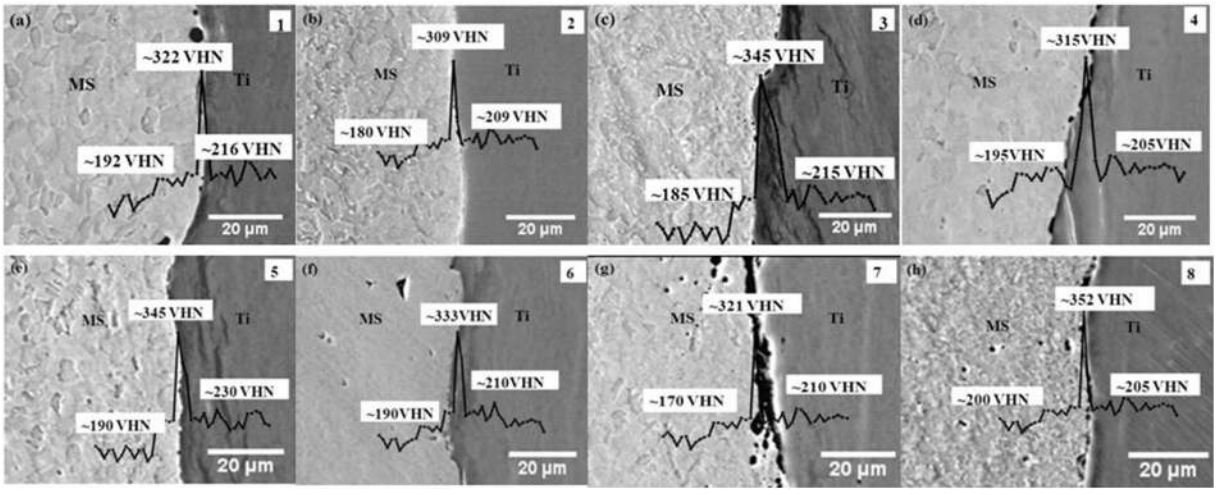

Fig. 2. a–h Back scattered electron (BSE) images obtained from cross section of the friction welds fabricated with different welding parameters (microhardness profiles are superimposed); inset shows the number of the trial run (refer Table 2).

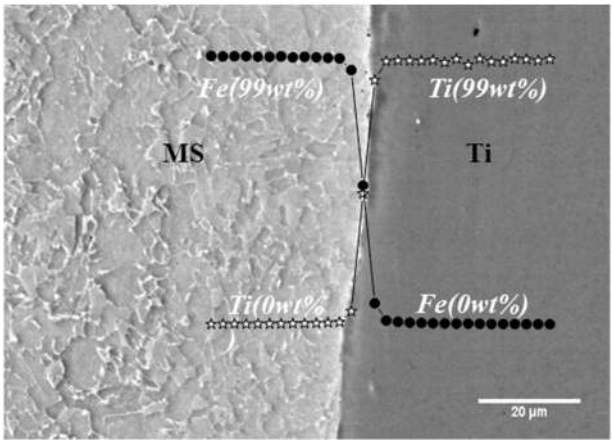

Fig. 3. BSE image of the MS/Ti friction joint fabricated with optimized welding parameters; concentration profile obtained across the joint interface is superimposed on the micrograph.

and have been used for fabrication of welds for detailed characterization and evaluation of mechanical properties, which are described in the subsequent sections.

3.2. Characterization of the friction weld joint:

3.2.1. Variation of microstructure, microchemistry and mechanical properties across the joint

Fig. 3 shows the BSE image of the MS/Ti friction joint fabricated with optimized parameters. It is evident from the micrograph that the interface is free from weld defects such as pores and irregularities. Elemental redistribution profiles obtained across the 'as welded' friction joint is superimposed on the micrograph. Smoothly varying error function type concentration profile, gives no indication for the formation of any secondary phases at the interface. Diffusing distances for Fe and Ti were estimated to be ~2 μm on either side of the interface. The cross over point was observed to be at a concentration of 48.5 wt% of Fe and 51.5 wt% of Ti, the concentration of which matches with the concentration of FeTi type intermetallic phase [5]. These concentration values were used as input to predict the phases that formed at the interface. To calibrate the conditions for simulation, the room temperature phases and the UTS values of MS and Ti base materials were initially predicted. Table 3 provides the volume fraction of phases and the ultimate tensile strength (UTS) predicted using JMatPro for the MS and Ti, which shows a close match with the experimental values. The same approach was followed to predict the phases and the properties in the 'as welded' joints, which are also presented in Table 3. Based on the simulations, the phases present at the interface can be summarized as αFe + FeTi + TiC with a considerable increase in the UTS value to ~670 MPa.

3.2.2. Confirmation of phases at the interface

Fig. 4 shows the XRD pattern obtained from the cross section of 'as welded' MS/Ti dissimilar joint. In addition to the parent phases (bcc-Fe and hcp-Ti), Bragg reflections were observed at 2θ positions of 43.5°, 49.6°, 59°, which correspond to (200), (202) and (210) planes of Fe_2Ti phase. Although unambiguous evidence was obtained for Fe_2Ti phase, the reflections corresponding FeTi phase could not be uniquely distinguished due to overlap with either the Fe_2Ti phase or αTi.

Fig. 5a shows a typical TEM bright field (BF) image obtained from the interface region of the friction weld. This consisted of isolated regions (shown by dotted circles in Fig. 5a) of different contrast. These isolated regions consisted of few fine sized particles ranging from 20 to 50 nm (arrow marked in Fig. 5b). The SAD pattern obtained from one such region is shown in Fig. 5c. Analysis of the electron diffraction pattern revealed overlapping ring and spot patterns along [$\bar{1}11$] and [$\bar{1}12$] zone axis for FeTi and bcc-Fe respectively thus confirming the prediction of intermetallic phase in 'as welded' MS/Ti joints.

Table 3
Comparison of the experimental and predicted values of UTS values.

Region	Volume fraction of phases	UTS(MPa)	
		Experimental	Predicted (this work)
Mild steel	Ferrite-0.98 Cementite-0.02	445	479
Interface	Ferrite-0.6 FeTi-0.3 TiC-0.1	–	669
Grade-2 Ti	Alpha Ti-1	325	334

3.3 Effect of thermal exposure on the weld

3.3.1. Evolution of interface microstructure with thermal exposure

Fig. 6a–d show the BSE images of the MS–Ti interface subjected to diffusion annealing at temperatures of 500, 600, 700 and 800 °C for 100 h with superimposed hardness profiles. Significant microstructural changes were observed at the interface and on the MS side of the joint with thermal exposure. At the lowest temperature i.e. 500 °C, grain size in regions up to a distance of ~530 μm from the interface was low (<10 μm) than those away from the interface (~15 μm). The microstructure beyond this resembled that of the starting material. The hardness on MS side was higher (212 ± 14 VHN) than that of the 'as received' material and was highest at the interface with an average value of ~274 ± 5 VHN.

At 600 °C additional features were observed on the MS side. Formation of a very thin zone (~0.8 μm width) at the interface (Fig. 6b) was observed which showed a relatively high hardness of ~285 ± 2 VHN, while the hardness gradually decreased from ~200 VHN in the vicinity of the interface to ~160 ± 11 VHN at a distance of about 1.5 mm from the interface. Width of this zone at the interface increased to ~2.6 μm with increase in temperature to 700 °C (shown by arrow Fig. 6c). Formation of coarse grains exceeding 120 μm was observed up to a distance of ~700 μm from the interface and the hardness reduced to very low values of ~109 ± 5 VHN in this region of the weldment. Beyond this distance the microstructure of the base metal is shown as an inset in Fig. 6c. At the highest temperature of 800 °C, thickness of the interface zone increased to nearly 4 μm. Coarse grained microstructure consisting of both ferrite and pearlite (shown by arrow in Fig. 6d)

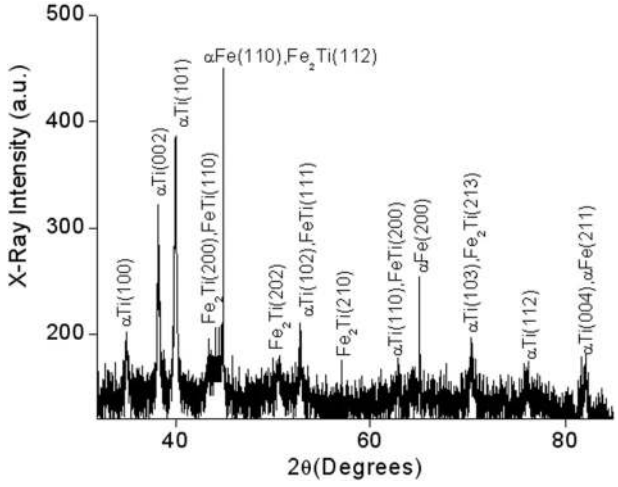

Fig. 4. XRD pattern obtained from the cross section of the 'as welded' MS/Ti dissimilar joint fabricated under optimized friction welding conditions.

existed throughout the thickness of the MS plate. Fig. 7 shows hardness of MS, Ti and interface regions separately plotted as a function of temperature. MS exhibits high hardness at 500 °C, which gradually reduces with increase in temperature and reaches the value as that of starting material. A decrease in the interface hardness with thermal exposure at 500 °C can be attributed to the recovery and recrystallisation of the deformed structure produced during the friction welding process. The continuous formation of brittle phases along the interface with increasing temperature is responsible for the increase in hardness at elevated temperatures.

3.3.2. Inter-diffusion across the Fe and Ti interface during thermal exposure

Concentration profiles obtained across the weld interface after thermal exposure are shown in Fig. 8a to d respectively. At 500 °C, the concentration profiles resembled the error function profiles with a maximum diffusion distance of ~3 μm. With increase in temperature, to 600 °C the diffusing distances for Fe and Ti in Ti side and MS side were obtained as ~2 and 3 μm, respectively. At the interface, the average chemical composition was obtained as 45.4 wt.% of Fe, 53.1 wt.% of Ti and 1.5 wt.% of C. Considerable increase in the concentration of C has been observed at the interface on Ti side at 700 °C (Fig. 8c). Composition at the cross over point was estimated as 64.2 wt.% Fe, 26.8 wt.% Ti and 9 wt.% C. At 800 °C, total width of the diffusion zone increased to ~8 μm due to increased inter-diffusion of the elements with temperature. The average composition in the C enriched region was obtained as 45.9 wt% Fe–42.5 wt% Ti–11.6 wt% C. At all the temperatures, Ti had higher diffusivity in bcc-Fe as compared to the diffusivity of Fe in hcp Ti. A comparison of the growth characteristics of the intermetallic zone is shown in Fig. 9. It is evident that the width of the zone in Fe–Ti systems fabricated by friction welding is ~4 μm as compared to diffusion bonding (10 μm) and explosive cladding (60 μm).

3.3.3. Prediction of phases at the MS/Ti joint interface

The change in microchemistry was used as an input to predict the formation of various phases at the interface of the MS/Ti joints heat treated at 500, 700 and 800 °C. Fig. 10a to c show the mole fraction (X) of phases predicted by JMatPro as a function of distance from MS to Ti across the interface at the three temperatures. At 500 °C, MC type of carbides ($X_{MC} = 0.4$) was observed at the interface in addition to the parent phases. High C concentration at the interface stabilized the γ phase of Fe, which was present at the interface at all the temperatures [17]. With increase in temperature to 700 °C, interface was found to consist of intermetallic phases such as FeTi and Laves (Fe_2Ti) (Fig. 10b). At the highest exposure temperature of 800 °C, a mixture of FeTi ($X_{FeTi} = 0.9$) and MC ($X_{MC} = 0.1$) type of carbides existed over a distance of ~3 μm from the interface (Fig. 10c).

3.3.4. Confirmation of diffusion aided secondary phases at the interface

The phases that formed due to thermal exposure of the weld cross section for 100 h at temperatures of 500 and 800 °C have been identified by X-ray diffraction patterns shown as Fig. 11a and b respectively. At 500 °C, Bragg peaks corresponding to Fe_2Ti intermetallic phases has been observed in addition to the parent phases and possibly FeTi also, whereas at a higher temperature of 800 °C apart from the above, reflections corresponding to TiC ($2\theta = 36.04^0$) was also observed.

In order to uniquely identify these phases TEM investigations were carried out on thin foil specimens extracted from the interface of the weld heat treated at a temperature of 800 °C for 100 h. Fig. 12a and b show the typical bright field image and the corresponding SAD Pattern from the circled region in Fig. 12a respectively. Particles having an

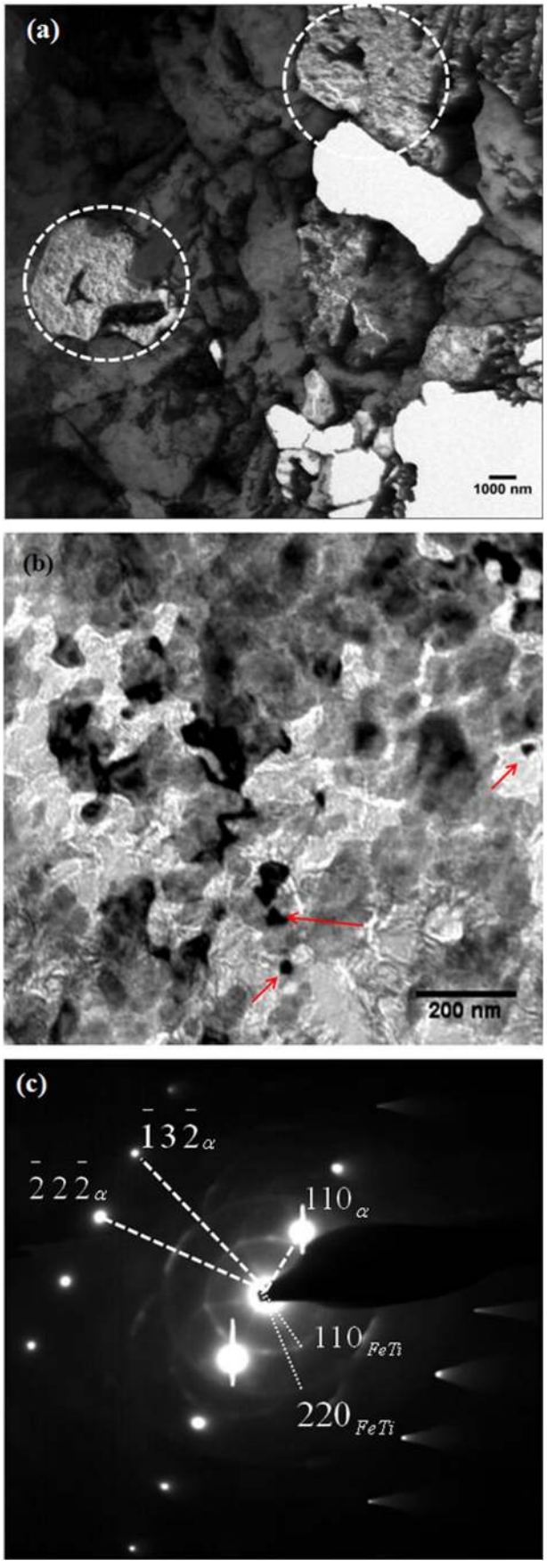

Fig. 5. a. TEM bright field image obtained from the interface of friction welded MS/Ti joints showing isolated regions (shown by dotted circle) with different contrast. b. Presence of fine particles of nm size in an magnified view of the isolated region circled in panel a. c. SAD pattern showing overlapping reflections from both bcc-Fe and FeTi phase along [$\bar{1}12$] and [$\bar{1}11$] zone axis respectively.

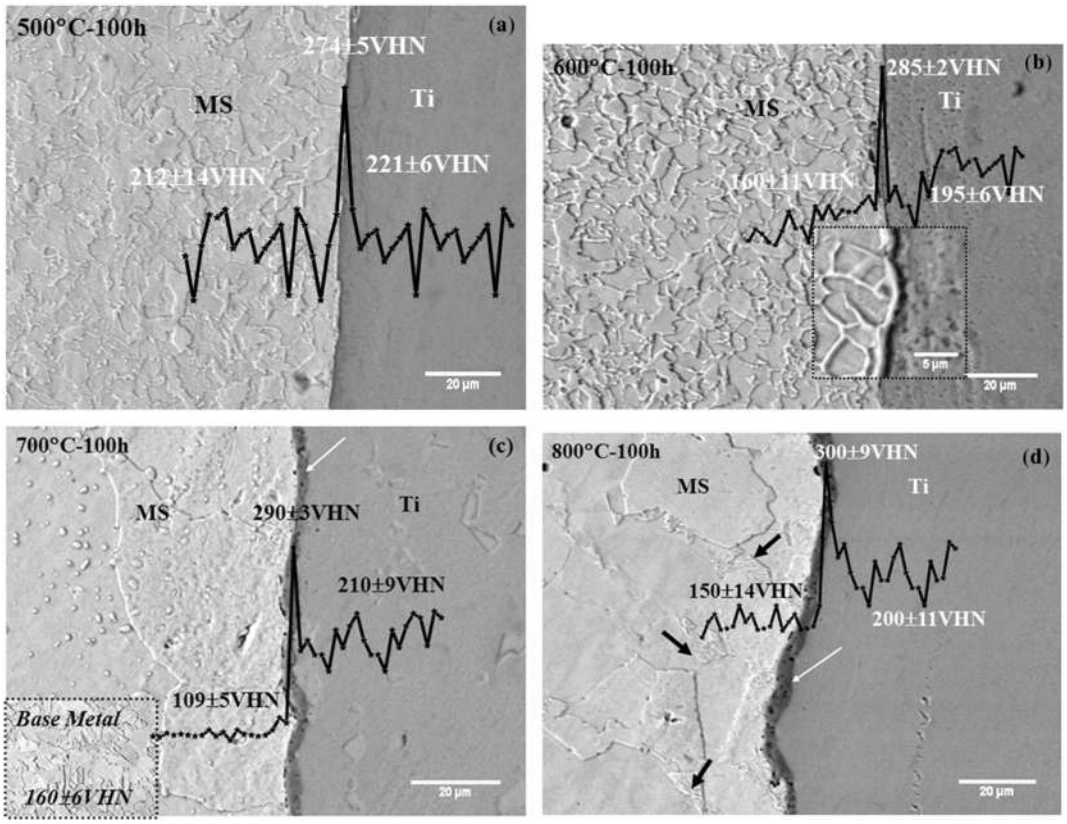

Fig. 6. BSE image showing the interface microstructure of MS/Ti friction joint with superimposed hardness profile after heat treated at a. 500 °C b. 600 °C; inset is the high magnification image of the interface c. 700 °C; inset is the base metal microstructure of mild steel and d. 800 °C for duration of 100 h respectively.

average size ~100 nm (circled in Fig. 12a) were observed throughout the interface. Analysis of the SAD pattern confirmed these particles to be intermetallic FeTi phase along [$\bar{1}11$] zone axis. Further the EDS spectrum in Fig. 12c taken from the circled particle showed that the Fe content is ~55.7 wt% and Ti is ~44.3 wt%. This composition shows that it corresponds to the FeTi phase [5] and the overestimation of Fe is attributed to the contribution from the MS matrix. Fig. 13a and b show the bright field image and SAD pattern obtained from another region with ~3 μm wide grain at the interface. Analysis of the SAD pattern identified the spot pattern to correspond to bcc Fe along [$\bar{1}12$] and ring pattern to fcc-TiC along [011] zone axis. Presence of TiC particles was further confirmed by obtaining a dark field image for [220] reflection (Fig. 13c).

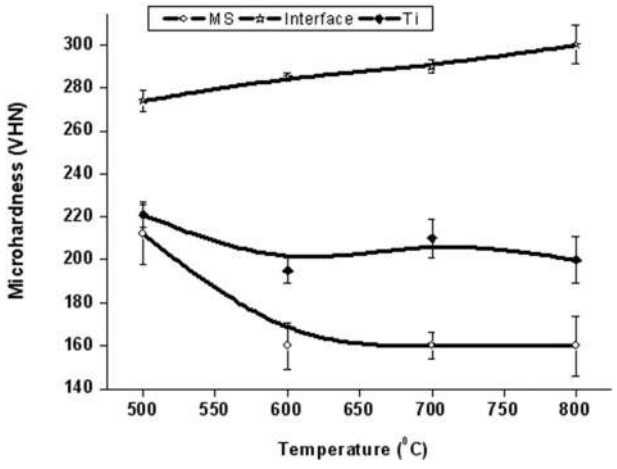

Fig. 7. A plot of hardness as a function of temperature.

3.3.5. Variation in mechanical property across the clad interface

In order to understand the effect of secondary phases on bond strength of the welds JMatPro calculations were carried out. Variation in the UTS has been predicted using the available information on temperature dependent variation in microchemistry, type and mole fraction of phases across the weld interface. Fig. 14a and b show the predicted UTS values at temperatures 500 and 800 °C plotted as a function of distance from the interface. The UTS value of the mild steel/Ti friction joints evaluated by JMatPro simulations show value of 496 MPa at 500 °C which agrees well with the reported value of 460 MPa for SS/Ti welds at 500 °C. However, the simulation shows that the UTS value reduces to ~110 MPa at 800 °C. Superimposing the measured composition on the ternary section of Fe–Ti–C system [17] at 800 °C the coexistence of FeTi, Fe_2Ti and TiC is observed which is provided as input for the JMatPro simulations, which explains for the above reduction. Simulation using only the FeTi phase as in a binary system [5] gives a value of UTS 285 MPa at 800 °C which compares well with the reported value of ~300 MPa [18].

The results of the study are summarized as follows:

- A good weld interface was obtained between MS and Ti using optimized friction welding parameters.
- Fine FeTi intermetallic phase was present in isolated regions at the weld interface.
- Inter-diffusion due to thermal exposure resulted in the formation of various secondary phases at the interface.
- Formation of a continuous layer of intermetallic phases was observed at the interface at temperatures above 600 °C by experimental and JMatPro computations.

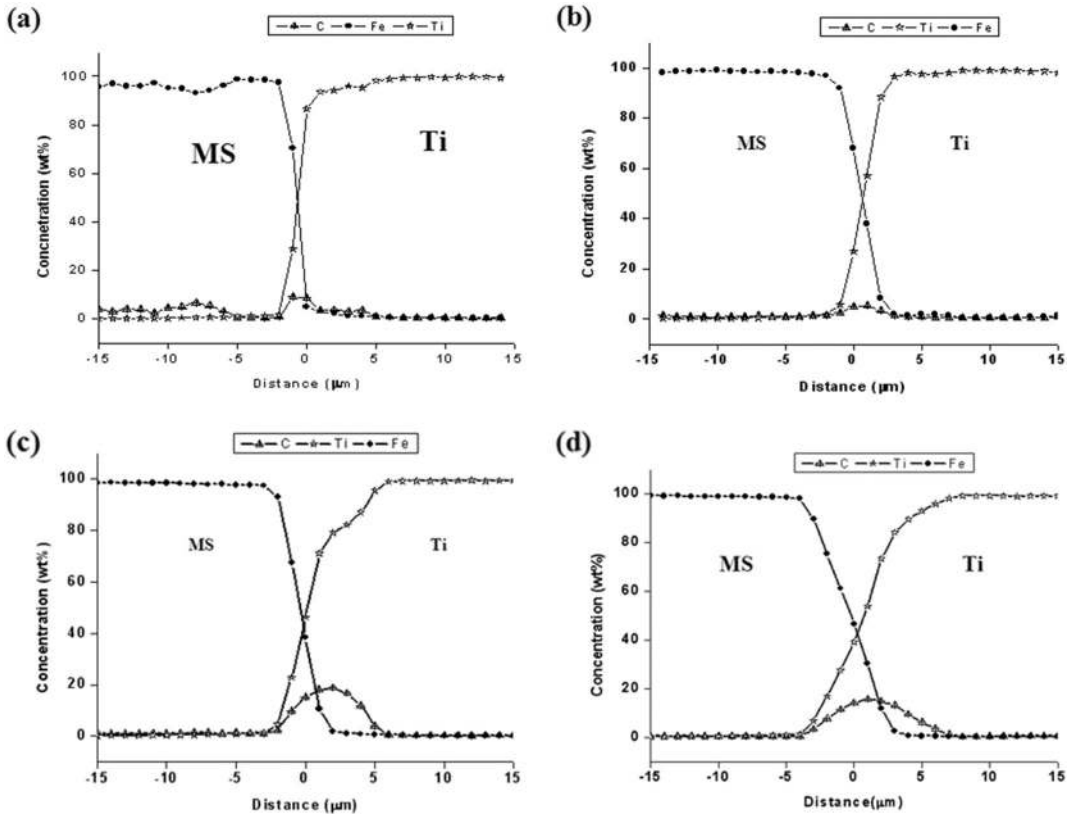

Fig. 8. Concentration profiles obtained across the MS/Ti friction joint heat treated at a. 500 °C b. 600 °C c. 700 °C and d. 800 °C for 100 h respectively.

- Bond strength of the MS/Ti friction joints was decreased significantly at high temperatures due to presence of brittle secondary phases.

4. Discussion

The choice of friction welding to obtain a bonded interface between MS and Ti, is based on the fact that it involves absolutely no melting of the base materials unlike fusion welding techniques, and further employs low temperatures unlike the diffusion bonding process which is carried out at high temperatures [11]. However, it is known that the interface microstructure is highly sensitive to the experimental parameters employed during welding. Hence, friction welding parameters were optimized through several trial runs. Changes occurring at the joint interface like the formation of pores, deformation of base materials and increase in hardness that may indicate insufficient bonding, degradation in properties and formation of intermetallic phases respectively were monitored to arrive at appropriate welding parameters.

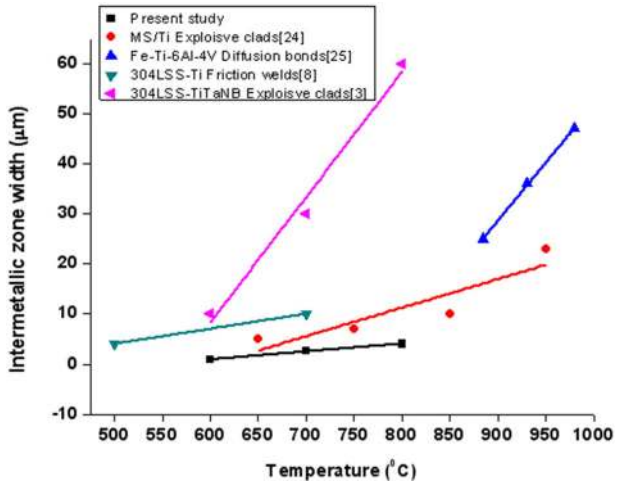

Fig. 9. Comparison of intermetallic zone width in Fe/Ti alloy systems.

In the 'as welded' MS/Ti joints, the presence of FeTi type of intermetallic phase at the interface (Fig. 5) has been unambiguously established. The intermetallic phase was present only as fine particles (≤50 nm) embedded in bcc-Fe matrix in isolated regions in contrast to its formation as a continuous zone parallel to the interface resulting in severe degradation of the bond strength of diffusion bonded joints [8,9]. Friction welding also did not result in the formation of deformation induced metastable phases in the base materials as observed in explosive clads [19]. Though temperature is not a variable parameter during friction welding high strain produced at the contact surfaces during welding leads to increase in temperature in localized regions [14,20]. This may lead to interdiffusion of alloying elements resulting in the formation of intermetallic phases. Intermetallic phases were observed in MS side of the joint since the diffusivity of Ti in bcc phase of Fe ($D_{Ti} = 5.5 \times 10^{-14}$ m^2/s at 900 °C) is higher than that of Fe in hcp-Ti ($D_{Fe} = 5 \times 10^{-15}$ m^2/s at 900 °C) [6]. However, the predicted UTS value was higher (~670 MPa) as compared to that of the reported values [16,18,21] suggesting that the presence fine intermetallic phases has no detrimental effect on the bond strength of the welds.

Observation of recrystallized structure during annealing at low temperature of 500 °C indicates high strain rates although no measurement of strain rate was carried out. However, comparison with literature where recrystallization temperature for low carbon steels experiencing strain rates in the range of 10^2 to 10^1/s is reported as 600 °C [22], it can

be expected that the strain rates involved in the present study is >1/s. ABAQUS based simulations in MS/MS friction welded joints also showed that the strain rate experienced by the weld zone is of the order of 1[14]. Plastic strain experienced by MS/Ti friction joints is expected to decrease the recrystallisation temperature of MS resulting in a fine grain structure with relatively high hardness. Though hardness at the interface was higher than the rest of the weldment (Fig. 6a) the presence of intermetallic phases could not be clearly established within the resolution limit of XRD (Fig. 11a).

With increase in temperature to 600 °C interdiffusion of alloying elements is enhanced resulting in increase in width of the region containing intermetallic phases (Fig. 6b). At a heat treatment temperature of 700 °C, recrystallized ferrite grains grow forming a coarse grained microstructure closer to the weld interface with relatively low hardness (Fig. 6c). At this temperature a continuous band of secondary phases were present based on the microstructural and microchemical analysis. Thermal exposure at 800 °C resulted in the formation of uniform sized ferrite grains with randomly distributed pearlite which is attributed to the heat treatment in $\alpha + \gamma$ phase field and subsequent transformation of γ to fine pearlite during cooling. This observation is in agreement with reported literature on friction welds of carbon steels [23,24].

As expected, width of the zone containing FeTi and Fe_2Ti type intermetallic phases increased with increase in temperature. MS/Ti joints showed sluggish diffusion kinetics as compared to Fe/Ti joints due to formation of TiC particles at the interface (Fig. 9). In addition confirmatory evidence was obtained for the formation of fine TiC (Fig. 13) precipitates at the weld interface. Contrary to this observation formation of a continuous layer of TiC precipitates has been reported [24] in Fe(0.16C)/Ti explosive clads after thermal exposure at 900 °C which was observed to decrease the mechanical strength of the joints. JMatPro

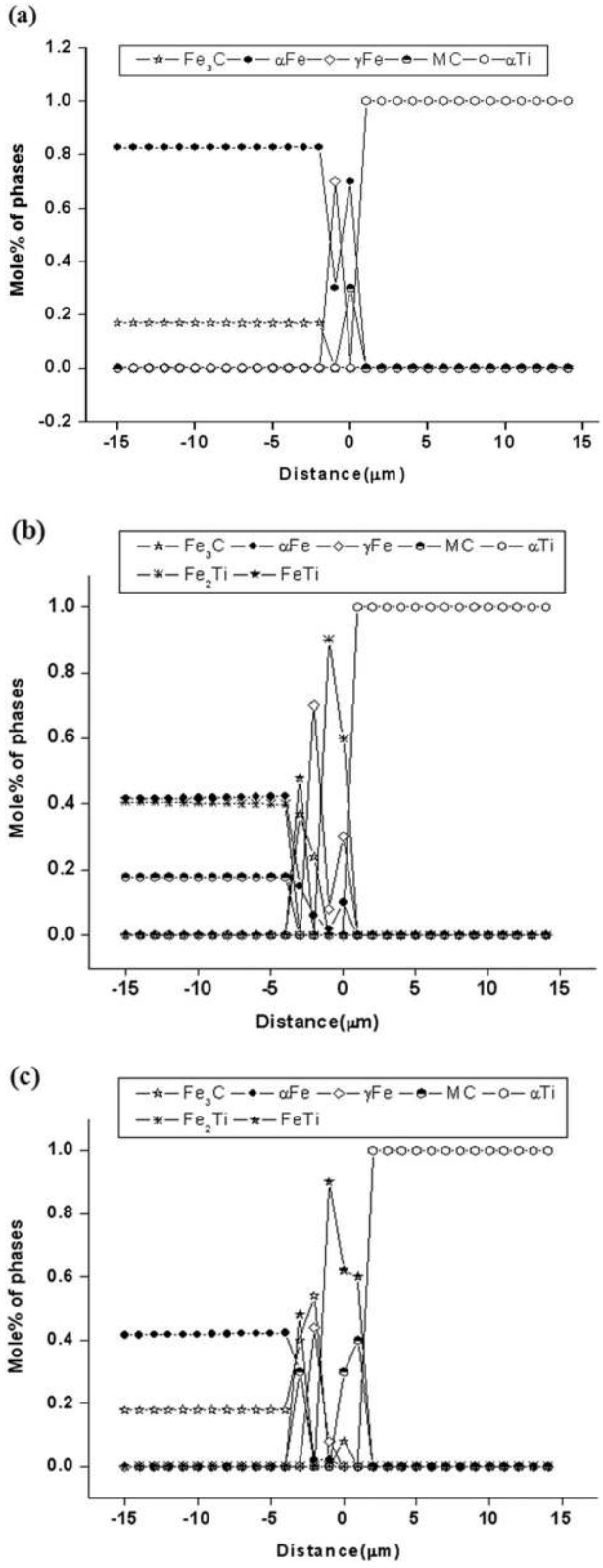

Fig. 10. Mole fraction of the phases predicted using JMatPro as a function of distance across the MS/Ti weld interface at a. 500 °C b. 700 °C c. 800 °C for 100 h respectively.

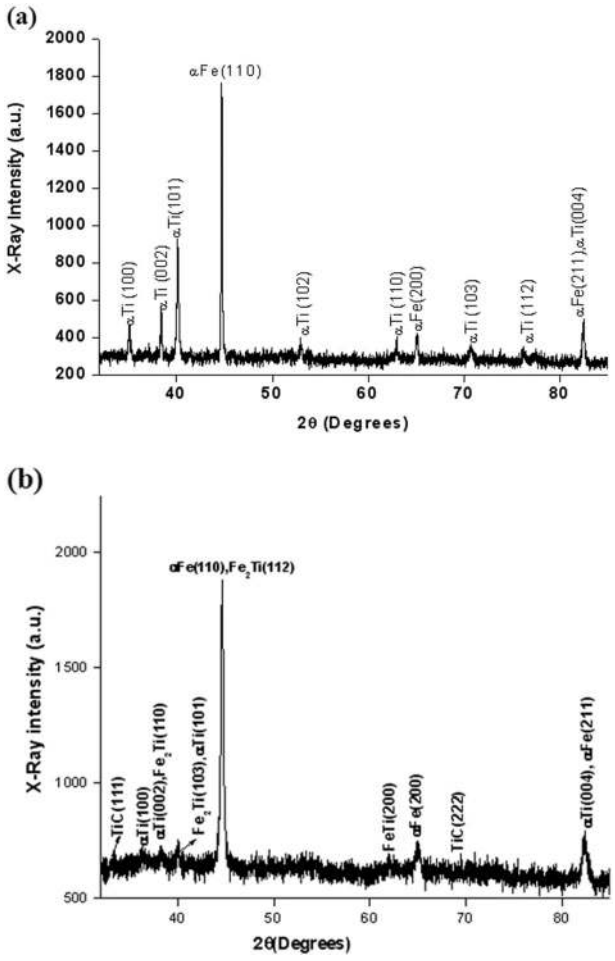

Fig. 11. XRD pattern obtained from the MS/Ti friction joint heat treated at a. 500 °C and b. 800 °C for 100 h respectively.

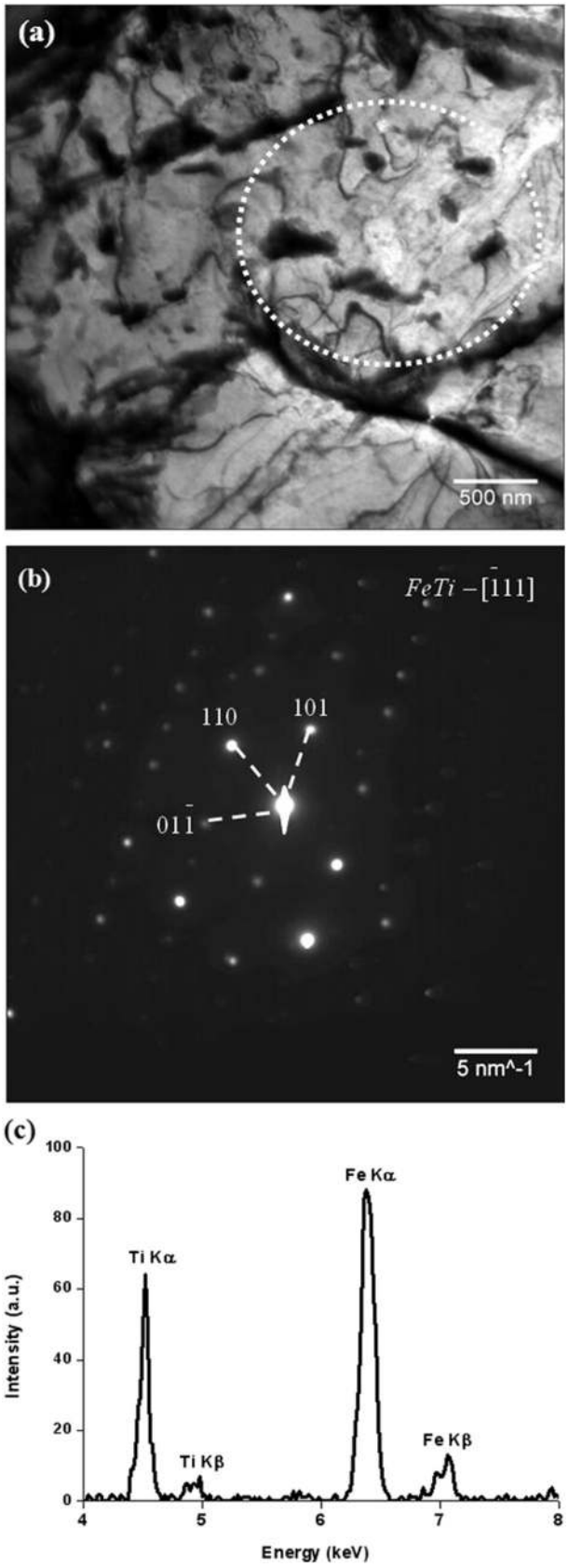

Fig. 12. a. TEM micrograph of the friction weld heat treated at a temperature of 800 °C for 100 h showing fine secondary phases. b. SAD pattern which is confirmatory for the presence of FeTi type intermetallic phase along [111]zone axis. c. EDS spectrum obtained from the circled region confirming the Fe and Ti rich nature of the phase.

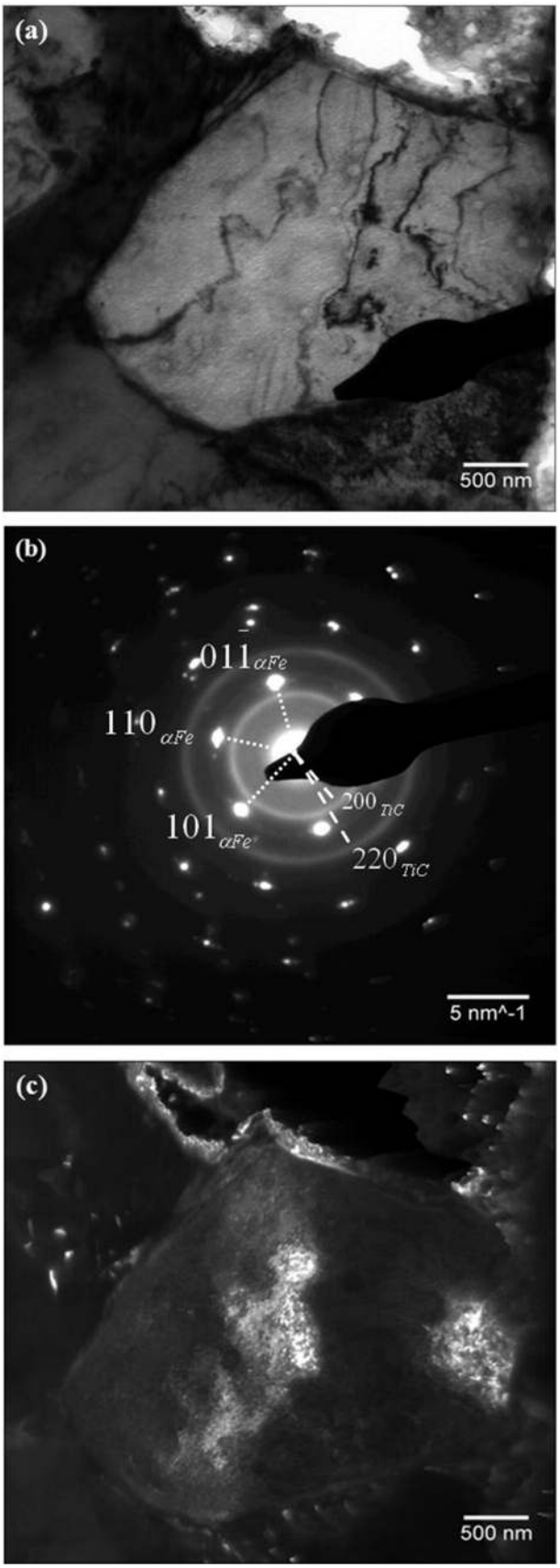

Fig. 13. a. TEM bright field micrograph showing an equiaxed grain of MS/Ti friction weld heat treated at a temperature of 800 °C for 100 h. b. SAD pattern having overlapping reflections from both bcc-Fe and TiC phase along [$\bar{1}$12] and [011] zone axis respectively. c. Dark field image corresponding to [220] reflection confirming the presence of TiC particles at the interface.

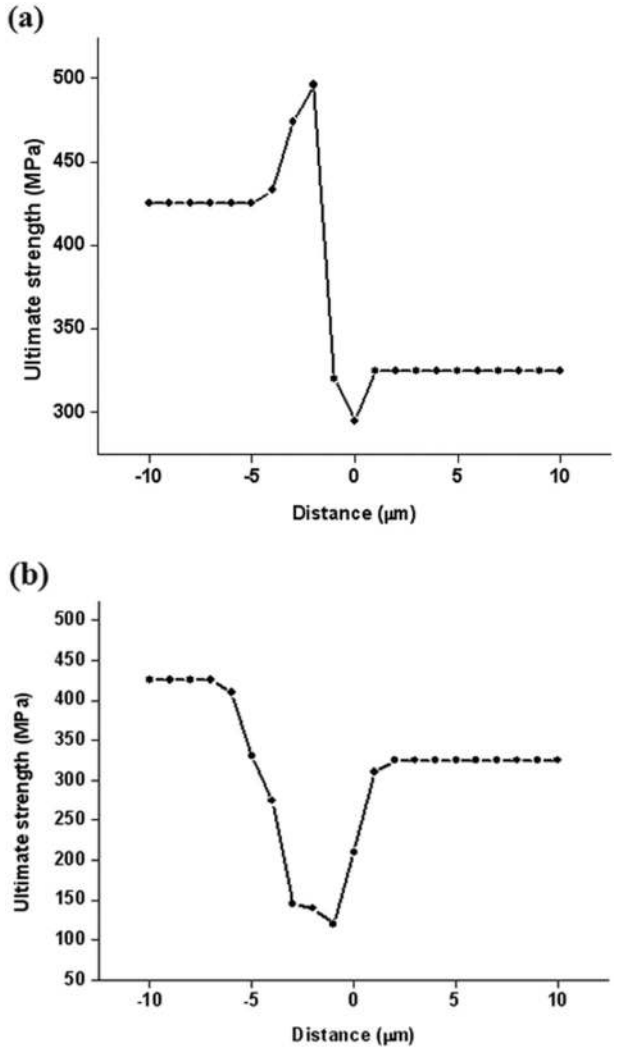

Fig. 14. Predicted UTS using JMatPro across the weld interface at a. 500 °C and b. 800 °C for 100 h respectively.

computations showed formation of γ phase of Fe at the interface which was not confirmed by the experimental results probably due to its finer size and also JMatPro® based simulations are carried out under equilibrium conditions.

A comparison of the experimental results on friction welding in this study with literature information on diffusion bonded joints and explosive clads [3,4,17,24–29], leads to the following inferences: (i) Intermetallic phases were present only as isolated particles in ferrite matrix as against a continuous zone parallel to the weld interface in diffusion bonded joints, (ii) few microns of deformation at the interface unlike deformation induced metastable phases over larger distances (~6 mm) in explosive clads, (iii) formation of very fine sized intermetallic phases as evidenced by ring and spot electron diffraction patterns unlike in explosive clads and (iv) limited diffusion zone of 6–7 μm even after heat treatment for 100 h as against ~330 μm in explosive clads heat treated for 20 h at 800 °C [3]. Formation of a continuous intermetallic zone reduced the strength of the joints considerably at this temperature of 800 °C (Fig. 14b).

During thermal exposure of these joints for various durations of 1–100 h in the temperature range of 500–700 °C, no significant change was observed at the interface up to 600 °C for short durations of 10 h, whereas the zone was observed at 20 h at this temperature. However, at 500 °C the formation of intermetallic zone was observed only for 100 h treatment. Hence, it is obvious that the duration of post weld heat treatments should be limited to 10 h in the range of 500–600 °C. Thus friction welding is a promising technique for joining Fe and Ti based alloys for industrial applications for specimen with suitable geometry.

5. Conclusions

- Friction welds of mild steel and grade-2 Ti have been successfully fabricated using optimized values of frictional force, upset force, burn-off length and rotational speed (0.8 tonnes, 1.6 tonnes, 3 mm and 1000 rpm respectively).
- Presence of fine FeTi intermetallic phase embedded in the ferrite matrix at the interface was confirmed by TEM investigations.
- Recrystallisation and grain growth in mild steel close to the interface was observed during diffusion annealing due to the plastic strain experienced during the friction welding process.
- At 600 °C and beyond resulted in the formation of different phases within the diffusion zone, the type of phases, their relative mole fraction and microchemical composition dictated by the temperature and time.
- JMatPro® based computations were carried out to predict the probable phases that would form at the joint interface during thermal exposure and consequential change in the mechanical properties due to presence of these secondary phases has been studied.
- Based on experimental results and JMatPro® based computations a maximum limit was set for post welding heat treatment conditions to avoid the formation of intermetallic phases at the joint interface.

Acknowledgements

The authors thank Dr. P.R. Vasudeva Rao, Director, IGCAR, Dr. T. Jayakumar, former Director, Metallurgy and Materials Group and Dr. M. Vijayalakshmi, Associate Director, Physical Metallurgy Group (PMG), IGCAR for their encouragement and support throughout the period of this work. The authors thank Mr. E. Mohandas and Mrs. M. Jyothi, PMG, IGCAR for XRD experiments. The Authors also thank Dr. Shyamprasad, Chief Scientist and Mr. V.D. Khedekar of National Institute of Oceanography, Goa for helping us with the EPMA experiments.

References

[1] B. Raj, U. Kamachi Mudali, Materials development and corrosion problems in nuclear fuel reprocessing plants, Prog. Nucl. Energy 48 (2006) 283–313.
[2] U. Kamachi Mudali, B.M. Ananda Rao, K. Shanmugam, R. Natarajan, B. Raj, Corrosion and microstructural aspects of dissimilar joints of titanium and type 304 stainless steel, J. Nucl. Mater. 321 (2003) 40–48.
[3] T.N. Prasanthi, C. Sudha, P.K. Parida, A. Dasgupta, S. Saroja, Prediction and confirmation of phases formed in the diffusion zone of Ti–5Ta–1.8Nb/304L SS explosive clads, Metall. Mater. Trans. A 46 (2015) 1519–1534.
[4] C. Sudha, T.N. Prasanthi, S. Saroja, M. Vijayalakshmi, Interdiffusion studies between Ti-5Ta-2Nb alloy and 304L austenitic stainless steel joined by explosive cladding process, in: S. Wang, et al., (Eds.), Proc. T.T. Chen Hon. Sym. Hydrometall. Electrometall. and Mater. Chara. John Wiley & Sons, USA, TMS, 2012 717.
[5] J.L. Murray, Phase diagrams of binary Ti alloys, ASM International, Metals park OH, 1987 99–111.
[6] B. Alemán, I. Gutiérrez, J.J. Urcola, Interface microstructures in diffusion bonding of titanium alloys to stainless and low alloy steels, Mater. Sci. Technol. 9 (1993) 633–641.
[7] http://www.engineeringtoolbox.com/linear-expansion-coefficients-d_95.html.
[8] M. Ghosh, S. Chatterjee, Diffusion bonded transition joints of titanium to stainless steel with improved properties, Mater. Sci. Eng. A 358 (2008) 152–158.
[9] M. Ghosh, S. Chatterjee, Characterization of transition joints of commercially pure titanium to 304 stainless steel, Mater. Charact. 48 (2002) 393–399.
[10] M. Ghosh, S. Chatterjee, Effect of interface microstructure on the bond strength of the diffusion welded joints between titanium and stainless steel, Mater. Charact. 54 (2005) 327–337.
[11] J.W. Elmer, D.D. Kautz, Lawrence, Fundamentals of Friction Welding, ASM Handbook, 6, ASM International, USA 1993, p. 504.
[12] S.D. Meshram, T. Mohandas, G. Madhusudhan Reddy, Friction welding of dissimilar pure metals, J. Mater. Process. Technol. 184 (2007) 330–337.

[13] Z. Guo, N. Saunders, J.P. Schillè, A.P. Miodownik, Material properties for process simulation, Mater. Sci. Eng. A 499 (2009) 7–13.
[14] S.A.A. Akbari Mousavi, A.R. Kelishami, Experimental and numerical studies of the effects of process parameters in the continuous friction welding process, Mater. Sci. Forum 580-582 (2008) 335–338.
[15] H.C. Dey, M. Ashfaqb, A.K. Bhaduri, K. Prasad Rao, Joining of titanium to 304L stainless steel by friction welding, J. Mater. Process. Technol. 209 (2009) 5862–5870.
[16] A. Fuji, T.H. North, K. Ameyama, M. Futamata, Improving tensile strength and bend ductility of titanium/AISI 304L stainless steel friction welds, Mater. Sci. Technol. 8 (3) (1992) 219–235.
[17] H. Ohtani, T. Tanaka, M. Hasebe, T. Nishizawa, Calculation of the Fe–C–Ti ternary phase diagram, Calphad 12 (3) (1988) 225–246.
[18] A. Fuji, K. Ameyama, T.H. North, Improved mechanical properties in dissimilar Ti–AISI 304L joints, J. Mater. Sci. 31 (1996) 819–827.
[19] C. Sudha, T.N. Prasanthi, V. Thomas Paul, S. Saroja, M. Vijayalakshmi, Metastable phase transformation in Ti–5Ta–2Nb alloy and 304L austenitic stainless steel under explosive cladding conditions, Metall. Mater. Trans. A 43 (2012) 3596–3607.
[20] M. Sahin, Characterization of properties in plastically deformed austenitic stainless steels joined by friction welding, Mater. Des. 30 (2009) 135–144.
[21] A.K. Lakshminarayana, V. Balasubramanian, An assessment of microstructure, hardness, tensile and impact strength of friction stir welded ferritic stainless steel joints, Mater. Des. 31 (2010) 4592–4600.
[22] N.A. Raji, O.O. Oluwole, Recrystallization kinetics and microstructure evolution of annealed cold-drawn low-carbon steel, J. Crystallization Process Technol. 3 (2013) 163–169.
[23] H. Fujii, L. Cui, N. Tsuji, M. Maeda, K. Nakata, K. Nogi, Friction stir welding of carbon steels, Mater. Sci. Eng. A 429 (2006) 50–57.
[24] H. Jiang, X. Yan, J. Liu, X. Duan, Effect of heat treatment on microstructure and mechanical property of Ti–steel explosive-rolling clad plate, Trans. Nonferrous Metals Soc. China 24 (2014) 697–704.
[25] B. Kurt, N. Orhan, E. Evin, A. Çali, Diffusion bonding between Ti–6Al–4V alloy and ferritic stainless steel, Mater. Lett. 61 (2007) 1747–1750.
[26] D.S. Bae, Y.R. Chae, S.P. Lee, J.K. Lee, S.S. Park, Y.S. Lee, S.M. Lee, Effect of post heat treatment on bonding interfaces in Ti/Mild steel/Ti clad materials, Procedia Engg. 10 (2011) 996–1001.
[27] Y. Morizono, M. Nishida, A. Chiba, T. Yamamuro, Effect of heat treatment on formation of columnar ferrite structure in explosively welded titanium/hypo eutectoid steel joints, Mater. Sci. Forum 465-466 (2004) 373–378.
[28] G.B. Kale, R.V. Patil, P.S. Gawade, Interdiffusion studies in titanium–304 stainless steel system, J. Nucl. Mater. 257 (1998) 44–50.
[29] S. Kundu, S. Sam, S. Chatterjee, Interface microstructure and strength properties of Ti–6Al–4V and microduplex stainless steel diffusion bonded joints, Mater. Des. 32 (2011) 2997–3003.